International Conference on Mathematics, Computational Methods & Reactor Physics (M&C 2009)
Saratoga Springs, New York, May 3-7, 2009, on CD-ROM, American Nuclear Society, LaGrange Park, IL (2009)

Comparison of Some Monte Carlo Models for Bound Hydrogen Scattering

T. M. Sutton*, T. H. Trumbull and C. R. Lubitz
Knolls Atomic Power Laboratory
P. O. Box 1072
Schenectady, 12301-1072
sutton@kapl.gov; trumbul@kapl.gov; lubitz@kapl.gov

ABSTRACT

Three approximate models for incoherent inelastic scattering of epithermal neutrons from ^{1}H bound in water are examined. The theoretical relationships between them are outlined, and the effects of using one versus another in Monte Carlo calculations are determined. A scattering law model based on the use of the short collision time approximation for downscattering, which simultaneously preserves detailed balance, gives the best results for the distribution of post-collision energies. For some criticality benchmark models, the differences in k_{eff} between the models can be as much as 50 pcm.

Key Words: Monte Carlo, incoherent inelastic scattering, epithermal neutron scattering

1. INTRODUCTION

In a series of two papers [1,2], Cullen, *et al.* have shown that the results of Monte Carlo calculations of nuclear systems that are sensitive to incoherent inelastic neutron scattering from hydrogen can vary dramatically depending on the particular combination of Monte Carlo code, nuclear data, and nuclear data processing code employed. Because the codes and the nuclear data libraries used to generate the results given in the papers differed in many ways, one could not use the results to isolate the differences due to the methods for treating incoherent inelastic scattering. In this paper, we compare three approximate models for treating incoherent inelastic scattering in the epithermal energy range for the case of ^{1}H bound in water molecules. By implementing the various models in the same code, we can focus solely on the differences in the results due to differences in the approximations.

Section 2 gives the theoretical background necessary to understand the three approximate models for incoherent inelastic scattering that we consider in this paper. Section 3 discusses how these approximate models may be used in Monte Carlo, and some details of their implementation in the MC21 code [3]. Section 4 presents some numerical results obtained using the models and Section 5 provides some concluding remarks.

* Corresponding author.

2. THEORETICAL BACKGROUND

2.1. Formulation of the Incoherent Inelastic Scattering Cross Section

Using the first Born approximation for the scattered neutron wavefunction and the Fermi pseudopotential to represent the neutron-nucleus interaction potential, it has been shown [4] quite generally that the double-differential scattering cross section may be written as

$$\sigma\left(E \to E', \mathbf{\Omega} \to \mathbf{\Omega}'\right) = \sigma_{\text{coh}}\left(E \to E', \mathbf{\Omega} \to \mathbf{\Omega}'\right) + \sigma_{\text{inc}}\left(E \to E', \mathbf{\Omega} \to \mathbf{\Omega}'\right), \tag{1}$$

In this expression, E and $\mathbf{\Omega}$ are the pre-collision neutron energy and direction vector, and the primed quantities are the post-collision values[1]. The two terms on the right side are the coherent and incoherent scattering cross sections, respectively, and are given by

$$\sigma_{\text{coh}}\left(E \to E', \mathbf{\Omega} \to \mathbf{\Omega}'\right) = \frac{\sigma_{\text{b,coh}}}{4\pi\hbar}\sqrt{\frac{E'}{E}}\frac{1}{2\pi}\int dt \int d\mathbf{r}\, e^{i(\boldsymbol{\kappa}\cdot\mathbf{r}-\omega t)} G\left(\mathbf{r},t\right) \tag{2}$$

and

$$\sigma_{\text{inc}}\left(E \to E', \mathbf{\Omega} \to \mathbf{\Omega}'\right) = \frac{\sigma_{\text{b,inc}}}{4\pi\hbar}\sqrt{\frac{E'}{E}}\frac{1}{2\pi}\int dt \int d\mathbf{r}\, e^{i(\boldsymbol{\kappa}\cdot\mathbf{r}-\omega t)} G_{\text{s}}\left(\mathbf{r},t\right), \tag{3}$$

where $\sigma_{\text{b,coh}}$ and $\sigma_{\text{b,inc}}$ are the bound coherent and incoherent scattering cross sections, $\hbar\boldsymbol{\kappa} = m\left(\mathbf{v} - \mathbf{v}'\right)$ is the momentum transfer vector, $\hbar\omega = E - E'$ is the energy transferred to the scatterer, m is the mass of the neutron, $\mathbf{r}$ is the position vector, $\mathbf{v}$ and $\mathbf{v}'$ are the pre- and post-collision neutron velocity vectors, and G and G_{s} are the time-dependent pair- and self-correlation functions.

The classical-mechanical interpretation of $G_{\text{s}}\left(\mathbf{r},t\right)d\mathbf{r}$ is that it is the probability that given a nucleus at the origin at time zero, the same nucleus will be in $d\mathbf{r}$ about $\mathbf{r}$ at time t. Similarly, $G\left(\mathbf{r},t\right)d\mathbf{r}$ is the probability that given a nucleus at the origin at time zero, the same or any other nucleus will be in $d\mathbf{r}$ about $\mathbf{r}$ at time t. The pair correlation function can thus be decomposed into self and distinct parts, *i.e.* $G = G_{\text{s}} + G_{\text{d}}$. For neutron inelastic scattering from liquids the distinct part may be neglected without significant error [5]. Furthermore, for protons $\sigma_{\text{b,coh}}$ is much smaller than $\sigma_{\text{b,inc}}$, so that we may make the incoherent approximation [6] and combine Eqs. (1)–(3) to obtain

$$\sigma\left(E \to E', \mathbf{\Omega} \to \mathbf{\Omega}'\right) = \frac{\sigma_{\text{b}}}{4\pi\hbar}\sqrt{\frac{E'}{E}}\frac{1}{2\pi}\int dt \int d\mathbf{r}\, e^{i(\boldsymbol{\kappa}\cdot\mathbf{r}-\omega t)} G_{\text{s}}\left(\mathbf{r},t\right). \tag{4}$$

[1] Unless explicitly stated otherwise, all quantities are given in the laboratory reference frame.

where the total bound cross section is given by $\sigma_b \equiv \sigma_{b,inc} + \sigma_{b,coh}$.

To understand the differences between the models we will consider, it is convenient to define several quantities. The intermediate scattering function[2] is defined as the spatial Fourier transform of G_s, i.e.,

$$\chi(\boldsymbol{\kappa}, t) = \int d\mathbf{r}\, e^{i\boldsymbol{\kappa}\cdot\mathbf{r}} G_s(\mathbf{r}, t), \tag{5}$$

and the dynamic structure factor is defined as the time Fourier transform of the intermediate scattering function, i.e.,

$$S(\boldsymbol{\kappa}, \omega) = \frac{1}{2\pi} \int dt\, e^{-i\omega t} \chi(\boldsymbol{\kappa}, t). \tag{6}$$

For isotropic media—such as liquids—the dynamic structure factor is independent of the direction of the momentum transfer vector. In this case, it is customary to define the alternative dimensionless variables

$$\alpha \equiv \frac{\hbar^2 \kappa^2}{2AmkT} = \frac{m|\mathbf{v} - \mathbf{v}'|^2}{2AkT} = \frac{E + E' - 2\mu\sqrt{EE'}}{AkT} \tag{7}$$

and

$$\beta \equiv -\frac{\hbar\omega}{kT} = \frac{E' - E}{kT}, \tag{8}$$

Where k is Boltzmann's constant, T is the ambient temperature, A is the scatterer-to-neutron mass ratio, and $\mu \equiv \boldsymbol{\Omega} \cdot \boldsymbol{\Omega}'$ is the cosine of the scattering angle. Changing variables from $(\boldsymbol{\kappa}, \omega)$ to (α, β) and multiplying by a factor of $kT/\hbar$, the asymmetric scattering law is defined as

$$\tilde{S}(\alpha, \beta) \equiv \frac{kT}{\hbar} S(\boldsymbol{\kappa}, \omega). \tag{9}$$

More commonly, however, one finds the incoherent inelastic scattering cross section given in terms of the symmetric scattering law

$$S(\alpha, \beta) \equiv e^{\beta/2} \tilde{S}(\alpha, \beta). \tag{10}$$

[2] This quantity should strictly be referred to as the incoherent intermediate scattering function to distinguish it from the coherent intermediate scattering function (the spatial Fourier transform of G). Since the incoherent approximation has been invoked, however, no confusion should exist due to this simplification in notation. The same discussion applies to the dynamic structure factor.

In the literature, this quantity is generally simply referred to as the scattering law, and we will follow that convention for the remainder of this paper. Combining Eqs. (4)–(6), (9) and (10) yields an expression for the double differential scattering cross section in terms of the scattering law, i.e.

$$\sigma\left(E \to E', \mathbf{\Omega} \to \mathbf{\Omega}'\right) = \frac{\sigma_b}{4\pi kT}\sqrt{\frac{E'}{E}}e^{-\beta/2}S\left(\alpha,\beta\right). \tag{11}$$

2.2. Detailed Balance

In general terms the principle of detailed balance [5] states that, for a physical system in thermodynamic equilibrium, the probability per unit time for transitioning from state *i* to state *j* multiplied by the density of states *i* is equal to the probability per unit time for transitioning from state *j* to state *i* multiplied by the density of states *j*. For thermal neutron scattering in an infinite, homogeneous, non-absorbing medium, this implies that

$$\phi\left(E\right)\sigma\left(E \to E', \mathbf{\Omega} \to \mathbf{\Omega}'\right) = \phi\left(E'\right)\sigma\left(E' \to E, -\mathbf{\Omega}' \to -\mathbf{\Omega}\right), \tag{12}$$

where

$$\phi\left(E\right) = \frac{E}{\left(kT\right)^2}e^{-E/kT} \tag{13}$$

is the Maxwellian flux spectrum corresponding to the ambient temperature, *T*. It is highly desirable that any model of the scattering law results in a scattering cross section that satisfies Eq. (12). By substituting Eq. (11) into Eq. (12), one can show that a necessary and sufficient condition for satisfying detailed balance is for the scattering law to be an even function of β.

2.3. Models of the Scattering Law

2.3.1. The monatomic ideal gas model

For many materials the self-correlation function may be well-represented using the Gaussian approximation [7]. In these cases, the intermediate scattering function takes the form

$$\chi\left(\boldsymbol{\kappa}, t\right) = e^{-\frac{\kappa^2}{2M}\gamma(t)}, \tag{14}$$

where *M* is the mass of the scatterer and $\gamma\left(t\right)$ is the width function. For a monatomic ideal gas (MIG), it may be shown [5] that $\gamma\left(t\right) = kTt^2 - i\hbar t$. Using Eqs. (6)–(10) yields the familiar result

$$S_{\mathrm{MIG}}(\alpha,\beta)=\frac{1}{\sqrt{4\pi\alpha}}e^{-\frac{\alpha^2+\beta^2}{4\alpha}}. \tag{15}$$

Since S_{MIG} is an even function of β, the monatomic ideal gas model satisfies detailed balance.

2.3.2. The effective temperature model

For a cubic Bravais lattice vibrating harmonically, the width function may be shown to be given by [7]

$$\gamma(t)=\hbar\int_0^\infty d\xi\,\frac{\rho(\xi)}{\xi}\left[\coth\left(\frac{\hbar\xi}{2kT}\right)\left(\cos(\xi t)-1\right)+i\sin(\xi t)\right], \tag{16}$$

where $\rho(\xi)$ is the phonon frequency distribution. We now employ the short-collision-time (SCT) approximation, in which the trigonometric functions in Eq. (16) are replaced by their series expansion up to the second-order terms in *t* [8]. Now, defining an effective temperature by

$$T^*(T)\equiv\frac{\hbar}{2k}\int_0^\infty d\xi\,\rho(\xi)\xi\coth\left(\frac{\hbar\xi}{2kT}\right), \tag{17}$$

the width function becomes $\gamma(t)=kT^*t^2-i\hbar t$, which has exactly the same form as that of the monatomic ideal gas with the effective temperature T^* replacing the ambient temperature *T*. Using Eqs. (6)–(10) yields

$$S_{\mathrm{ET}}(\alpha,\beta)=\frac{1}{\sqrt{4\pi\alpha\dfrac{T^*(T)}{T}}}e^{-\left(\frac{(\alpha+\beta)^2}{4\alpha}\frac{T}{T^*(T)}-\frac{\beta}{2}\right)}, \tag{18}$$

where the "ET" subscript denotes the use of the effective temperature. Substitution of Eq. (18) into Eq. (11) yields a double differential scattering cross section which is identical to that of a monatomic ideal gas in thermal equilibrium at the effective temperature T^*. It has been shown [5] that the SCT approximation as used here suffers from two difficulties. First, S_{ET} is not symmetric in β, and thus the cross section does not satisfy detailed balance at the ambient temperature *T*. Second, while it is a good approximation for downscattering, it does not represent upscattering correctly.

2.3.3. The short collision time model

It has been demonstrated [8] that the ET scattering law can be modified so as to satisfy detailed balance while simultaneously taking advantage of the SCT approximation's accuracy at modeling downscattering. The modification is

$$S_{\mathrm{SCT}}(\alpha,\beta) \equiv S_{\mathrm{ET}}(\alpha,-|\beta|) = \frac{1}{\sqrt{4\pi\alpha\dfrac{T^*(T)}{T}}} e^{-\left(\frac{(\alpha-|\beta|)^2}{4\alpha}\frac{T}{T^*(T)}+\frac{|\beta|}{2}\right)}. \tag{19}$$

As can be seen, this function is symmetric in β—thus satisfying detailed balance, and is identical to S_{ET} for negative β—thus preserving the SCT approximation for downscattering.[3]

3. USING THE SCATTERING LAW IN CONTINUOUS ENERGY MONTE CARLO

For certain moderator nuclides—including ^{1}H bound in water molecules—scattering law data are available in ENDF/B [9] and similar nuclear databases. These data are tabulated on a mesh in (α,β) space and are given for various temperatures. Using interpolation laws, the tabulated data may be used to construct the double differential scattering cross section and quantities derived from it. In computing some of these quantities—e.g., integrated scattering cross sections and scattering kernels—it is often necessary to integrate over portions of (α,β) space that are outside of the limits of the tabulated mesh. For this purpose, approximate analytical models of the scattering law—such as those discussed in §2.3 above—may be employed. Codes such as NDEX (which processes nuclear data for MC21), FLANGE-II [8] and others use Eq. (19) for this purpose. The use of tabulated scattering law data (supplemented when needed by analytical approximate models) is typically confined to the thermal energy range.

Another use of approximate scattering law models—and the one of interest in this paper—is to treat the kinematics of scattering in the epithermal energy range. In principle, the expressions for the scattering laws given by Eqs. (15), (18) and (19) could be used along with Eq. (11) to create probability distribution functions (PDFs) from which post-collision neutron parameters could be sampled. In practice, however, it is more convenient to use equivalent analog methods. In these, the proton pre-collision velocities are first sampled from an appropriate distribution function. Then, the neutron-proton system is transformed to a center-of-mass (COM) reference frame and the kinematics of the collision are computed. Finally, the post-collision neutron velocity is transformed back to the original reference frame. The details of this process for the three theoretical models under consideration are given below.

3.1. The Monatomic Ideal Gas Model

First consider the case of a monatomic ideal gas of scattering nuclei with number density *N* and temperature *T*. For a neutron moving with velocity **v**, the scattering rate per unit volume with nuclei with velocities in *d***V** about **V** is

$$R(\mathbf{V}|\mathbf{v},T) = \sigma_0|\mathbf{v}-\mathbf{V}|\varphi(\mathbf{V}|T), \tag{20}$$

[3] Even though the short collision time approximation was used to derive the scattering laws given by both Eqs. (18) and (19), we use the "SCT" designation for that given by Eq. (19) to be consistent with the previous literature.

where σ_0 is the scattering cross section which is assumed to be independent of the relative velocity, and

$$\varphi\left(\mathbf{V}\middle|T\right) \equiv \left(\frac{M}{2\pi kT}\right)^{3/2} e^{-\frac{MV^2}{2kT}} \tag{21}$$

is the Maxwellian velocity distribution. The target velocity PDF for a neutron colliding with pre-collision velocity **v** is thus given by

$$p_{\text{Maxwell}}\left(\mathbf{V}\middle|\mathbf{v},T\right) = \frac{\sigma_0}{C}\left|\mathbf{v}-\mathbf{V}\right|\varphi\left(\mathbf{V}\middle|T\right), \tag{22}$$

where

$$C \equiv \left(\int d\mathbf{V} R\left(\mathbf{V}\middle|\mathbf{v},T\right)\right) \tag{23}$$

is the normalization constant.

MC21 uses Gelbard's algorithm [10] for sampling from p_{Maxwell}. Since Ref. 10 is not widely available, the algorithm will be outlined here. A nearly identical algorithm is used in the MCNP code [11]. We begin by factoring the target velocity PDF as

$$p_{\text{Maxwell}}\left(\mathbf{V}\middle|\mathbf{v},T\right) = f_1\left(\mathbf{V}\right) f_2\left(\mathbf{V}\right), \tag{24}$$

where

$$\begin{aligned} f_1\left(\mathbf{V}\right) &\equiv \frac{\sigma_0\left|\mathbf{v}-\mathbf{V}\right|}{C\left(v+V\right)} \\ f_2\left(\mathbf{V}\right) &\equiv \left(v+V\right)\varphi\left(\mathbf{V}\middle|T\right) \end{aligned}, \tag{25}$$

and v and V are the neutron and target nucleus speeds. Any PDF of the form of Eq. (24) may be sampled [12] by first sampling a provisional target velocity $\mathbf{V}^*$ from the PDF

$$q\left(\mathbf{V}^*\right) \equiv \frac{f_2\left(\mathbf{V}^*\right)}{\int d\mathbf{V} f_2\left(\mathbf{V}\right)}. \tag{26}$$

The provisional target velocity is accepted as the actual target velocity with probability

$$\begin{aligned} \rho &= f_1\left(\mathbf{V}^*\right) \big/ \hat{f}_1 \\ \hat{f}_1 &= \max f_1\left(\mathbf{V}\right) \end{aligned} . \tag{27}$$

From Eq. (26) one may obtain

$$\begin{aligned} q\left(\mathbf{V}^*\right) &\equiv a\varphi\left(\mathbf{V}^* \middle| T\right) + \left(1-a\right) q'\left(\mathbf{V}^*\right) \\ a &= \frac{v}{v + \left\langle V \right\rangle} \\ q'\left(\mathbf{V}^*\right) &= \frac{V^*}{\left\langle V \right\rangle} \varphi\left(\mathbf{V}^* \middle| T\right) \\ \left\langle V \right\rangle &\equiv \int d\mathbf{V}\, \mathbf{V} \varphi\left(\mathbf{V} \middle| T\right) = \sqrt{\frac{8kT}{\pi M}} \end{aligned} . \tag{28}$$

In Gelbard's algorithm, the provisional target velocity is sampled from the Maxwellian velocity distribution with probability a, otherwise it is sampled from q'. Algorithms for sampling from the Maxwellian distribution are well known (see, for example, Ref. 12). To obtain an algorithm for sampling from q', begin by changing from a velocity variable to the dimensionless energy variable $\varepsilon = MV^2 \big/ 2kT$. The corresponding PDF is

$$\tilde{q}\left(\varepsilon\right) = \varepsilon e^{-\varepsilon} . \tag{29}$$

Given two pseudorandom numbers ξ_1 and ξ_2 drawn on the unit interval, ε may be sampled from the PDF given by Eq. (29) using $\varepsilon = -\ln\left(\xi_1 \xi_2\right)$. The provisional target velocity is then obtained as

$$\mathbf{V}^* = \sqrt{\frac{2\varepsilon kT}{M}} \mathbf{\Omega}^* , \tag{30}$$

where $\mathbf{\Omega}^*$ is a unit vector sampled from an isotropic distribution.

Once the target velocity has been determined, a transformation is made into the COM reference frame, the collision analyzed using standard methods, and the post-collision quantities transformed back to the laboratory reference frame (see, for example, Ref. 13).

3.2. The Effective Temperature Model

The algorithm just described for the MIG model may also be used for the ET model simply by sampling the target velocity from $p_{\text{Maxwell}}\left(\mathbf{V}\middle|\mathbf{v},T^*\left(T\right)\right)$ rather than from $p_{\text{Maxwell}}\left(\mathbf{V}\middle|\mathbf{v},T\right)$. The other steps are unchanged.

3.3. The Short Collision Time Model

There is an analog algorithm—also due to Gelbard [10]—that corresponds to the SCT model given by Eq. (19). Again, since Ref. 10 is not widely available, it will be outlined here. Since for downscattering the SCT model is identical to the ET model, we have

$$\sigma_{\text{SCT}}\left(E\to E'\middle|T\right)=\sigma_{\text{ET}}\left(E\to E'\middle|T\right),\ E'<E\,. \tag{31}$$

To obtain an equivalent expression for upscattering, we begin by recalling from §2.3.2 that the ET model for the scattering law evaluated at the ambient temperature *T* results in a scattering cross section equivalent to a monatomic ideal gas at the effective temperature T^*, i.e.

$$\sigma_{\text{ET}}\left(E\to E'\middle|T\right)=\sigma_{\text{MIG}}\left(E\to E'\middle|T^*\right), \tag{32}$$

where we have explicitly denoted the temperature at which the scattering laws (and thus corresponding cross sections) are evaluated. The ET scattering cross section thus satisfies the detailed balance relation

$$\phi\left(E\middle|T^*\right)\sigma_{\text{ET}}\left(E\to E'\middle|T\right)=\phi\left(E'\middle|T^*\right)\sigma_{\text{ET}}\left(E'\to E\middle|T\right), \tag{33}$$

Since the SCT model preserves detailed balance at the ambient temperature and since Eq. (31) holds for downscattering, for upscattering it is necessary that

$$\phi\left(E\middle|T\right)\sigma_{\text{SCT}}\left(E\to E'\middle|T\right)=\phi\left(E'\middle|T\right)\sigma_{\text{ET}}\left(E'\to E\middle|T\right),\ E'>E\,. \tag{34}$$

Solving Eq. (33) for $\sigma_{\text{ET}}\left(E'\to E\middle|T\right)$ and substituting into Eq. (34) results in

$$\begin{aligned}\sigma_{\text{SCT}}\left(E\to E'\middle|T\right)&=\frac{\phi\left(E'\middle|T\right)\phi\left(E\middle|T^*\right)}{\phi\left(E\middle|T\right)\phi\left(E'\middle|T^*\right)}\sigma_{\text{ET}}\left(E\to E'\middle|T\right)\\&=\exp\left[-\left(E'-E\right)\left(\frac{1}{T}-\frac{1}{T^*}\right)\right]\sigma_{\text{ET}}\left(E\to E'\middle|T\right),\quad E'>E.\end{aligned} \tag{35}$$

We may thus write

$$\sigma_{\mathrm{SCT}}\left(E \to E' \middle| T\right) = p_{\mathrm{accept}}\sigma_{\mathrm{ET}}\left(E \to E' \middle| T\right), \tag{36}$$

where

$$\begin{aligned} p_{\mathrm{accept}} &= 1, && E' < E \\ &= \exp\left[-\left(E'-E\right)\left(\frac{1}{T}-\frac{1}{T^*}\right)\right], && E' > E \end{aligned} \tag{37}$$

Since the right-hand-side of Eq. (36) is the product of two factors, the same rejection technique used for Eq. (24) may be employed. Gelbard's algorithm begins by sampling post-collision neutron parameters as described in §3.1 and §3.2. In this case, however, these are treated as provisional. If the result is downscattering, then the provisional results are always accepted ($p_{\mathrm{accept}} = 1$). If the result is upscattering, however, then the provisional values are retained with probability $p_{\mathrm{accept}} = \exp\left[-\left(E'-E\right)\left(1/T - 1/T^*\right)\right]$. If the provisional values are not retained, then new provisional post-collision parameters are sampled using the ET model and the rejection process applied to these. This entire process is repeated until a set of post-collision parameters is accepted.

3.4. Usage of Scattering Law Models in Various Monte Carlo Codes

The MC21 code classifies all nuclides as either moderators or non-moderators, where a moderator is any nuclide for which tabulated thermal scattering data is given in ENDF/B File 7. For ^{1}H bound in water, MC21 uses the tabulated scattering law data from 10^{-5} eV to the top of the thermal range. From the top of the thermal range to 20 MeV the SCT model is used. For other moderators the SCT model is used from the top of the thermal range to 400 *kT*. For non-moderators the MIG model is used from 10^{-5} eV to 400 *kT*. Above 400 *kT* all target nuclei except ^{1}H are treated is if they were at rest.

The procedures used by the MCNP code [11] are the same as for MC21, with the important exception that the MIG model is used for all cases for which MC21 uses the SCT model. In the epithermal energy range, the VIM code [10] uses the SCT model for ^{1}H bound in water and the MIG model for other moderators. The RCP01 code [14] uses a modified version of the ET model. In the RCP01 method, post-collision neutron parameters are sampled using the ET model. If, however, this results in upscattering then the post-collision energy is set equal to the pre-collision energy instead; otherwise the ET results are retained.

4. RESULTS

To compare the various approximate scattering law models, we use each to sample the distribution of fractional neutron energy change for 4.09 eV neutrons scattering from ^{1}H bound in water at 293.6 K. As a reference solution, we use a fractional energy change PDF obtained by integrating Eq. (11) over the scattering cosine using the procedures described by Ballinger [15]. The scattering law used for this purpose was computed by LEAPR [16] and obtained from

ENDF/B File 7. For comparison, sampled fractional-energy-change frequencies were generated using the three approximate models for the scattering law: S_{MIG}, S_{ET}, and S_{SCT}.

Figures 1 and 2 show the sampled frequencies superimposed on the reference solution (ENDF: black line). As can been seen, all three approximate models fail to capture the quasi-elastic peak and associated structure of the PDF corresponding to small energy changes. In addition, the use of the MIG model (MIG: blue line) causes too many neutrons to lose almost all of their energy in a collision, but as expected does a good job in treating the upscattering. Use of the ET model with $T^* = 1368$ K (ET: pink line) does a good job of treating large fractional energy losses, but substantially over-predicts upscattering. The use of the SCT model (SCT: yellow line) does as well as the ET model for large fractional energy losses, and as well as the MIG model for upscattering.

It is also of interest to know what effect the use of various approximate models for the scattering law can have on k_{eff}. Figure 3 shows the difference in k_{eff} between the use of the SCT and MIG approximations to the scattering law in the epithermal energy range for a set of 32 benchmark calculations from the LEU-SOL-THERM series [17]. The SCT approximation consistently predicts a lower value than the MIG approximation. The differences range between 18 and 50 pcm, with an average difference of 28 pcm. The largest difference is for the SHEBA-II experiment, which is an unreflected assembly fueled with an aqueous solution of 5%-enriched uranyl fluoride.

Finally, it should be mentioned that the additional CPU time required for the SCT model versus the MIG model is negligible.

5. CONCLUSIONS

Three approximate models of the neutron scattering law for ^{1}H bound in water were examined. In one model, denoted MIG, the hydrogen atoms are treated as if they were a monatomic ideal gas at the ambient temperature. The second model employs the short collision time approximation to account for the effects of the chemical binding of the proton in the water molecule. This model is referred to as the ET model as it is equivalent to a monatomic ideal gas at an effective temperature. The third model, denoted SCT, employs the short collision time approximation for downscattering, and uses a relationship based on the principle of detailed balance to treat upscattering. The SCT model is superior to the other two in treating neutron energy change due to collisions with ^{1}H bound in water in the epithermal energy range. The SCT model was also shown to yield smaller k_{eff} values than the MIG model for one class of thermal benchmark problems.

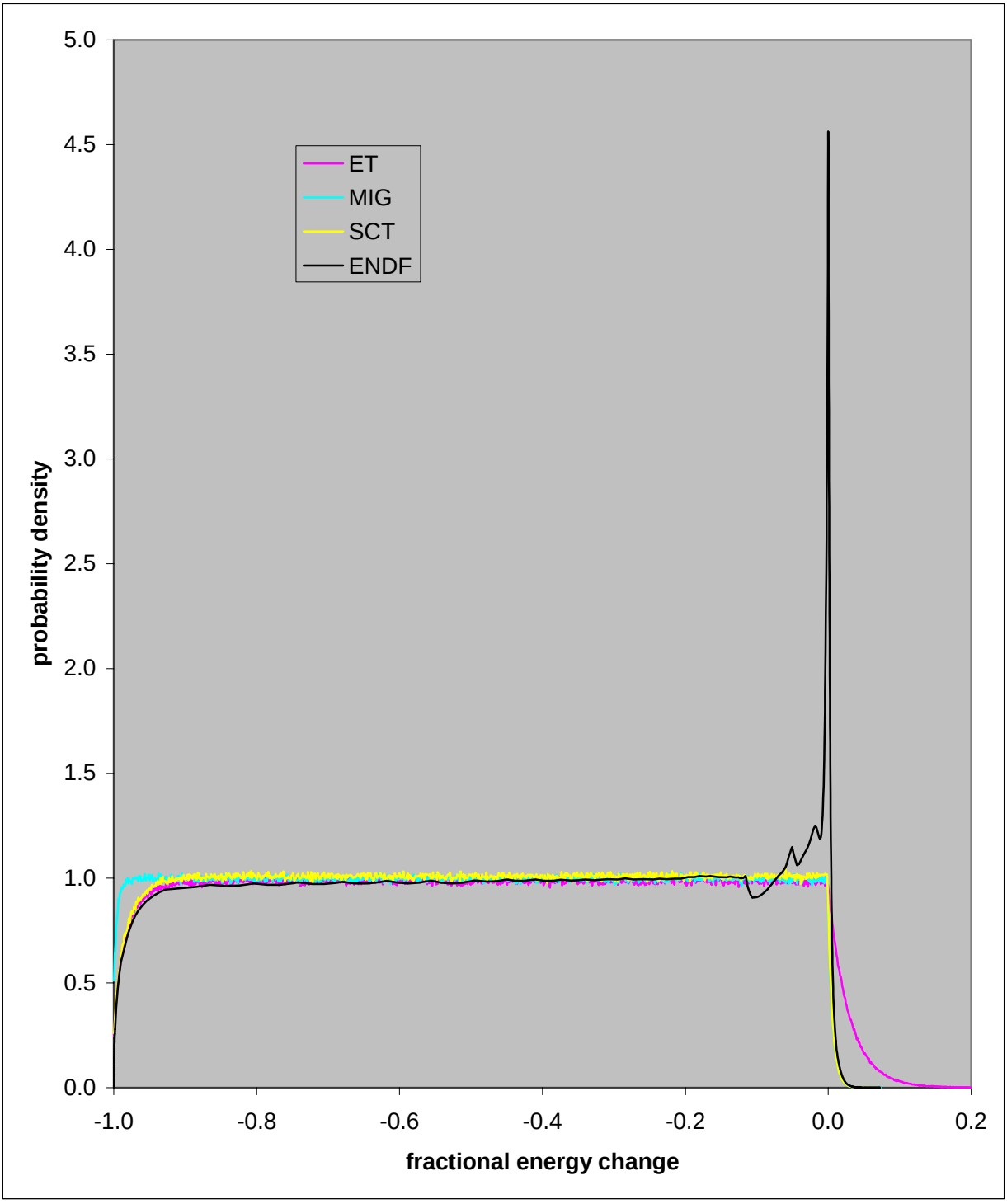

Figure 1. Fractional Energy Change PDF for 4.09 eV Neutrons on ^{1}H in Water at 293.6 K

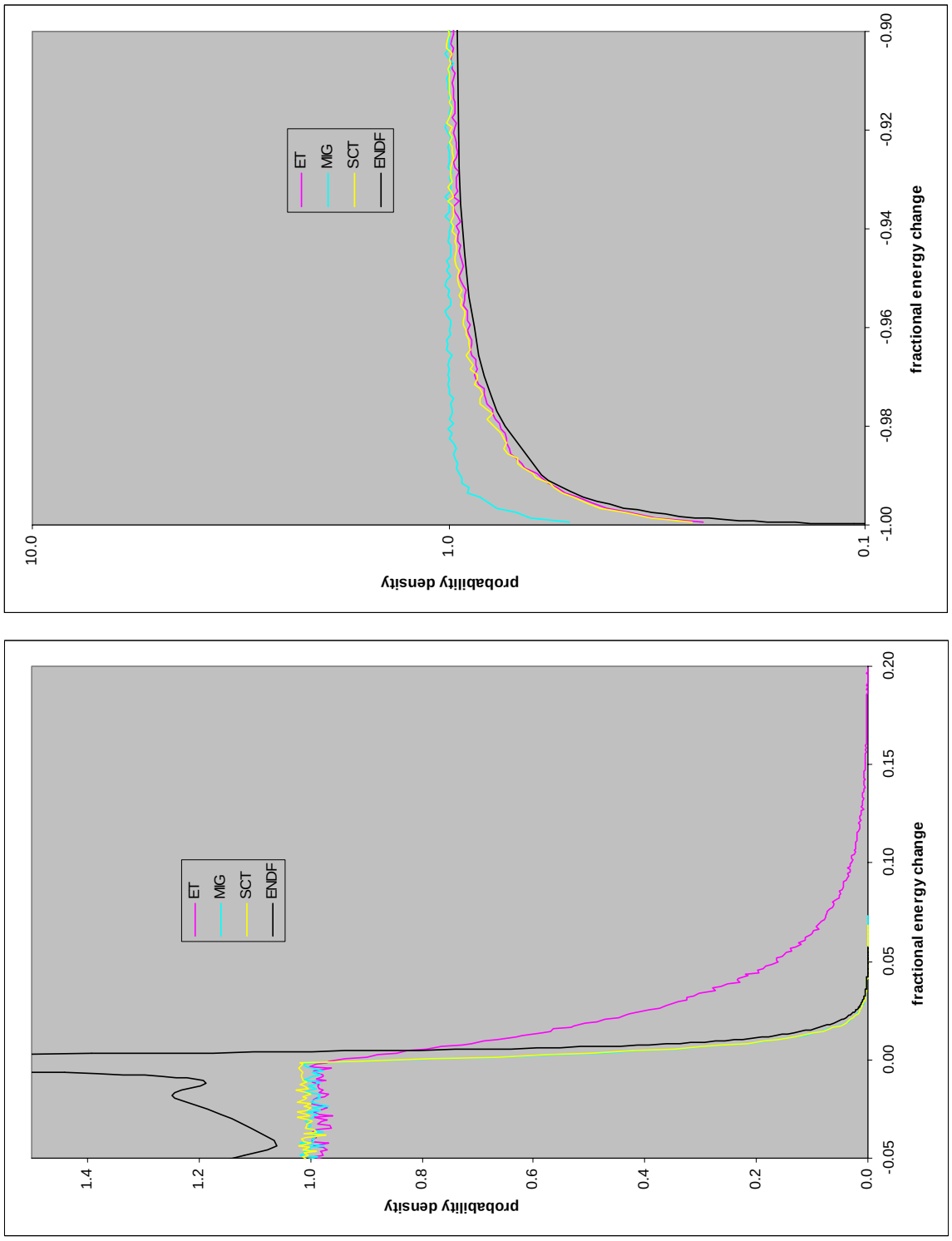

Figure 2. Fractional Energy Change PDF for 4.09 eV Neutrons on ^{1}H in Water at 293.6 K (details)

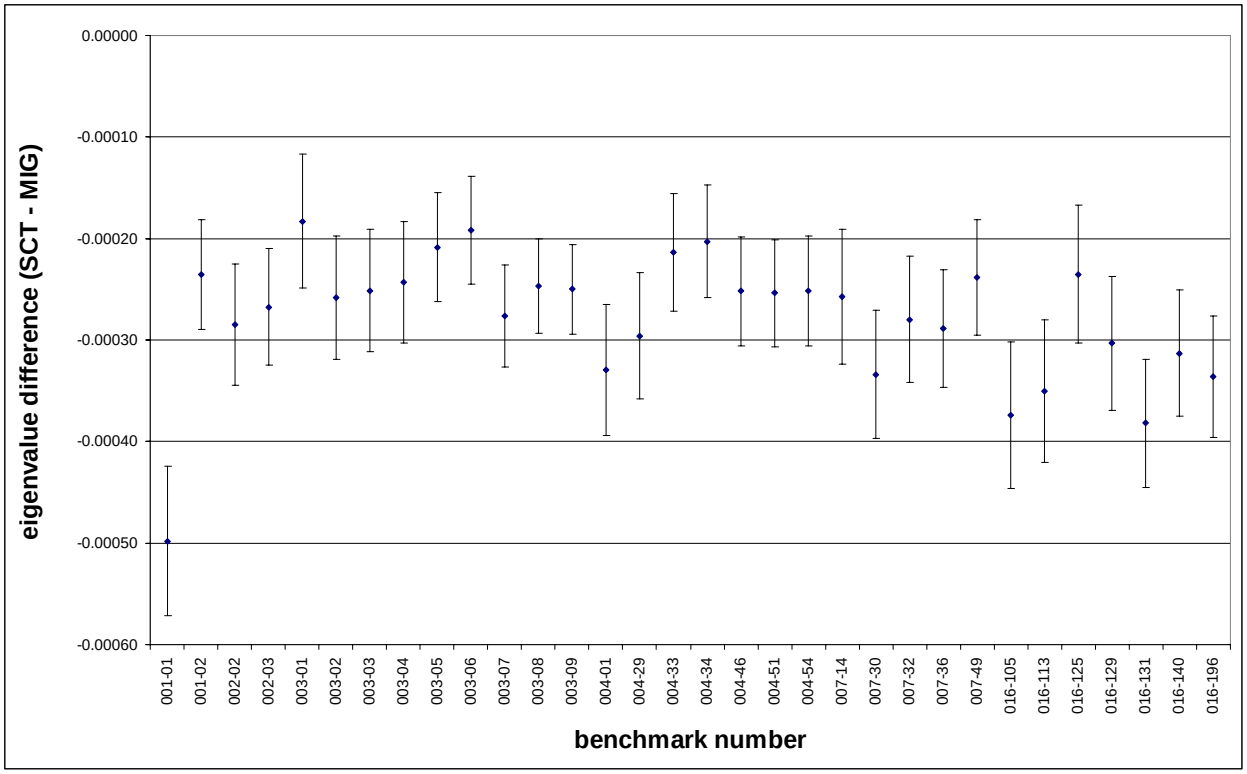

Figure 3. LEU-SOL-THERM Eigenvalue Differences Between SCT and MIG Epithermal Scattering Models

ACKNOWLEDGMENTS

The authors would like to acknowledge Dr. D. P. Griesheimer (Bettis Atomic Power Laboratory), who programmed the original epithermal scattering treatment for MC21, and Mr. P. S. Dobreff (Knolls Atomic Power Laboratory), who generated the benchmark results.

REFERENCES

1. Dermott E. Cullen, *et al.*, "How Accurately Can We Calculate Thermal Systems," UCRL-TR-203892, Lawrence Livermore National Laboratory (2004).
2. Dermott E. Cullen, *et al.*, "How Accurately Can We Calculate Neutrons Slowing Down in Water," UCRL-TR-220605, Lawrence Livermore National Laboratory (2006).
3. T. M. Sutton, T. J. Donovan, T. H. Trumbull, P. S. Dobreff, E. Caro, D. P. Griesheimer, L. J. Tyburski, D. C. Carpenter and H. Joo, "The MC21 Monte Carlo Transport Code", *Proc. Joint Int. Topical Meeting on Mathematics & Computation and Supercomputing in Nuclear Applications*, Monterey, California, USA, April 15–19 (2007).
4. Léon Van Hove, "Correlations in Space and Time and Born Approximation Scattering in Systems of Interacting Particles," *Phys. Rev.*, **95**, pp. 249–262 (1954).
5. M. M. R. Williams, *The Slowing Down and Thermalization of Neutrons*, John Wiley & Sons, New York, USA (1966).

6. George I. Bell and Samuel Glasstone, *Nuclear Reactor Theory*, Van Nostrand Reinhold, New York, USA (1970).
7. S. N. Purohit, *Neutron Scattering and Thermalization Lectures*, S-333, Aktiebolaget Atomenergi (1963).
8. G. M. Borgonovi, *Neutron Scattering Kernel Calculations at Epithermal Energies*, GA-9950, Gulf General Atomic, San Diego, USA (1970).
9. M. Herman, ed., *ENDF-6 Formats Manual: Data Formats and Procedures for the Evaluated Nuclear Data File ENDF/B-VI and ENDF/B-VII*, BNL-NCS-44945-05-Rev. (ENDF-102), Brookhaven National Laboratory (2005).
10. E. M. Gelbard, "Epithermal Scattering in VIM," FRA-TM-123, Argonne National Laboratory (1979).
11. X-5 Monte Carlo Team, *MCNP – A General Monte Carlo N-Particle Transport Code, Version 5*, LA-UR-03-1987, Los Alamos National Laboratory (2003).
12. C. J. Everett and E. D. Cashwell, "A Third Monte Carlo Sampler," LA-9721-MS, Los Alamos National Laboratory (1983).
13. E. D. Cashwell and C. J. Everett, "A Practical Manual on the Monte Carlo Method for Random Walk Problems," LA-2120, Los Alamos Scientific Laboratory (1957).
14. L. A. Ondis II, L. J. Tyburski, and B. S. Moskowitz, *RCP01 – A Monte Carlo Program for Solving Neutron and Photon Transport Problems in Three-Dimensional Geometry with Detailed Energy Description and Depletion Capability*, B-TM-1638, Bettis Atomic Power Laboratory (2000).
15. C. T. Ballinger, "The Direct $S(\alpha,\beta)$ Method for Thermal Neutron Scattering," *Proc. Int. Conf. on Mathematics and Computation, Reactor Physics, and Environmental Analysis*, **1**, 134, Portland, Oregon USA, April 30–May 4 (1995).
16. R. E. MacFarlane, *New Thermal Neutron Scattering Files for ENDF/B-VI Release 2*, LA-12639-MS (ENDF-356), Los Alamos National Laboratory (1994).
17. NEA Nuclear Science Committee, *International Handbook of Evaluated Criticality Safety Benchmark Experiments*, **IV**, 34, NEA/NSC/DOC(95)03, Organization for Economic Co-operation and Development/Nuclear Energy Agency (2005).